

Open Access Article

FLEXURAL BEHAVIOR OF FLY ASH BASED GEOPOLYMER REINFORCED CONCRETE T - BEAMS HAVING TRANSVERSE WEB OPENINGS

Mustafa Adel Saeed

Civil Engineering Department, Mustansiriyah University, Baghdad, Iraq/ Master student.

Ali Sabah Al Amlı

Civil Engineering Department, Mustansiriyah University, Baghdad, Iraq/ PHD.

Abstract

Because of the massive CO₂ emissions associated with cement manufacture, it is the primary cause of global warming. As a result, the writers and research organizations are motivated in multiple ways to find long-term solutions to this problem. The primary binder in geopolymer concrete is created by alkali activation some source materials such as fly ash, metakaoline, rice husk ash, and pulverized granulated blast furnace slag. Geopolymer concrete frequently has mechanical strength characteristics that are comparable to conventional concrete. The properties of the utilized source materials and the molar concentrations of the alkali activator, however, limit the application of this form of concrete. In this method, the relevant structural behavior can be studied. In addition, it is common that the transverse web openings may cause a relevant lack in structural behavior due to the inherent reduction of concrete within the existing section. The current study tries to investigate the flexural behavior of fly ash based geopolymer concrete by implementing an experimental program. Such program included casting and testing five fly ash geopolymer concrete T beams till failure. All the tested beams within this experimental program are of center to center span of 1600 mm and 1750 mm total length. The section dimensions are of total height of 250mm and flange width of 200mm while the while the web width is 100mm. The results showed that a lack of structural behavior can result from the presence of a transverse web opening in the center of geopolymer RC beams. The first cracking load, yielding load, and maximum load carrying capacity are all reduced when transverse web openings are present. In addition, the general performance of geopolymer T beams that have circular transverse web openings perform better than those that have square transverse web opening.

Keywords (in English): Geopolymer, fly ash, metakaoline, slag, reinforced concrete beams and Structural Behavior..

1.Introduction

In practice, the construction industry consumes a lot of energy and generates a lot of garbage. This is a major issue in terms of global warming and harmful environmental consequences. Because of its enormous carbon dioxide (CO₂) emissions, the cement sector plays a significant role in these issues¹. In this way, the seeking for another alternatives that can compensate cement is a serious task for the authors within civil engineering field. “Geopolymers” are such materials can be synthesized by the

Received: April ,24 , 2022 / Revised: May ,17, 2022 / Accepted: 21,May , 2022 / Published: 10 , June, 2022.

About the authors :Mustafa Adel Saeed

Email:

alkali activation of any suitable alomino-silicate materials such as slags, metakaoline, fly ash and red mud 2 and 3.

The resulted matrix of “Geopolymerization Process” is a hardened matrix that can play the same role of ordinary Portland cement (Primary Binders). In order to manufacture asequate and stable geopolymers, the source materials must be highly reactive, easy to release aluminum and having moderate water consumption. Many materials can be used as alkali activators such as Sodium Hydroxide (NaOH), Potassium Silicate (K_2SiO_3), Sodium Silicate (Na_2SiO_3) and Potassium Hydroxide (KOH) 4.

However, since the hardened matrix having good mechanical strength, stiffness and durability properties, geopolymer concrete can be reinforced to play the same role of conventional reinforced concrete within civil engineering applications.

1.2 Geopolymerization

In normal conditions and circumstances, $[SiO_4]^-$ and $[AlO_4]^-$ tetrahedral units become free once the alomino– silicate reaction is dissolved, and these units are then bonded together inside the polymeric precursor, releasing oxygen atoms. The bonding structure of $Si-O-Al-O$ is generated as a result. The chemical reactions of geopolymerization are described by the chemical formulas below 4.

It is worth to mention that the released water during the intended reaction is usually play a good role for workability and facilitates handling. However, this opposites the role of ordinary Portland cement when high level of water consumption can be noticed during the entire process of hydration⁵. Figure 1 illustrates this process schematically.

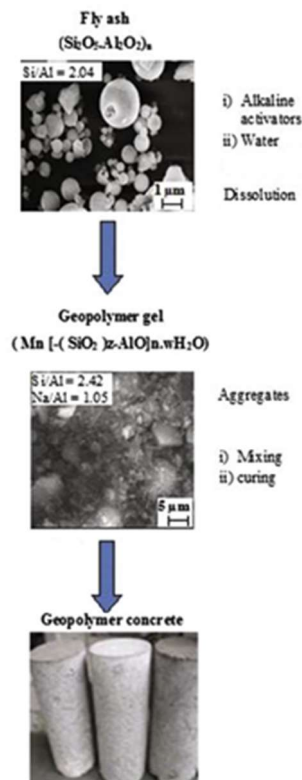


Figure 1. Geopolymerization process, schematic representation [4].

1.3 Study Significance

Getting reliable experimental results on the flexural behavior of geopolymer reinforced geopolymer T-beams is a critical issue for any researcher who wants to understand the relationship between the inherent mechanical properties of geopolymer concrete and the consequent structural behavior of these beams. So, this study tries to introduce a useful contribution within this field of research.

2. Materials and Methods

2.1 Materials

2.1.1 Fly Ash

The Class F fly ash that provided from “EUROBUILD” construction chemicals company was used within the present study as a source material for manufacturing GC which is shown in Plate (3-1). In addition, the X-Ray Fluorescence (XRF) testing was done in the National Center of Construction Laboratories and Researches (NCCLR) according to BS EN 196-2-2013 and the results shown in Table (3-1)

Table 1 XRF Analyses results of fly ash*

Composition Name	Composition	
	Chemical symbol	Weight %
Silica	SiO ₂	47.67
Alumina	Al ₂ O ₃	27.73
Alumina	Al ₂ O ₃	27.73
Lime	CaO	5.11
Magnesia	MgO	2.65
Sulfur salts in term of SO ₃	When C3A < 3.5%	/
	When C3A > 3.5%	0.34
Insoluble residue	IR	/
Loss on ignition	LOI	2.39
Tri-calcium Aluminate	C3A	42.38
Chloride	Cl	/

*The National Center of Construction Laboratories and Researches (NCCLR) conducted this examination.

2.1.2 Sand

The sand used within the current study is “Al-Ekhaider natural sand” which is of 4.75mm maximum size for being the fine aggregate within mixes. The grading of such aggregate was illustrated within Figure 2. The required test of this sand was done in the according to Iraqi specification No.45/1984 within the laboratories of the Engineering Consulting Office / University of Al - Mustansiriyah.

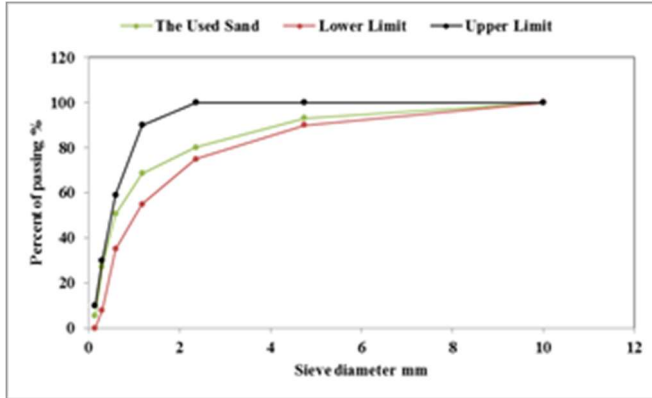


Figure 2. Sieve analyses of the used sand

2.1.3 Gravel

The 10mm maximum sized gravel that used within the present experimental program was brought from “AL-Nibaey” to be used as coarse aggregate within the mix. Such gravel was washed and air dried then stored by suitable containers till the date of testing, at that date, the gravel would be saturated “surface dried” before using. Figure 3 shows the grain size distribution of that gravel. The required test of this sand was done in the according to (B.S 882/1992) within the laboratories of the Engineering Consulting Office / University of Al - Mustansiriyah.

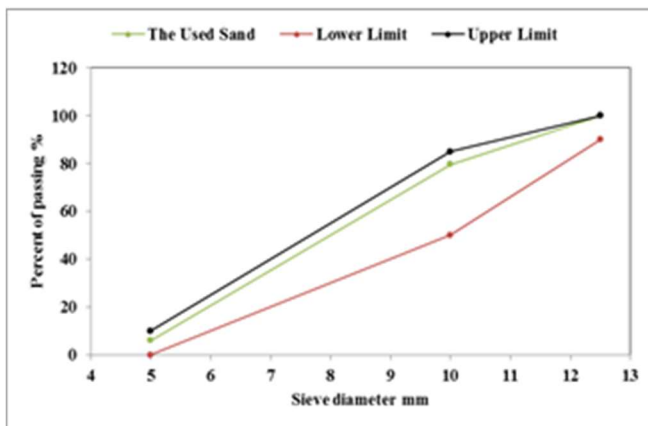


Figure 2. Sieve analyses of the used gravel

2.1.4 Sodium Hydroxide NaOH

The commercial NaOH solid slakes “Provided from Al Kout projects company“ that were 98% pure and packed in 25 kg sealed containers was used within this study. The solvent of “sodium hydroxide” liquid is initially set by melting flakes to prepare the alkaline solution; the volume of “NaOH flakes”

in the solution varies depending on the concentration that works needed. For this work, three solutions prepared with molar 10 M. This arbitrarily done by using NaOH flakes “314 g”, respectively to make “(1kg) of the solution”.

Table 2 Properties Sodium Hydroxide*

Components	Specification ASTM E291- 09	Results
Sodium hydroxide (NaOH)%	>97.5	98.14
Sodium chloride (NaCl)ppm**	<200	70
Sodium carbonate (Na ₂ CO ₃)%	<0.40	0.36
Sulphate as Na ₂ SO ₄ (ppm)	<200	70
Iron as Fe ⁺³ (ppm)	< 10	4.5
Copper as Cu ⁺² (ppm)		0.1
Nickel as Ni ⁺² (ppm)	<5	2.42
Manganese as Mn ⁺² (ppm)		0.02
Silicate as SiO ₂ (ppm)	<20	14
Water Insoluble (ppm)	<200	60

* According to Manufacturer.

**Ppm: part per million according to manufacturer.

2.1.5 Sodium Silicate Na₂SiO₃

Hal chemicals company sodium silicate or (glass water) is commercially available for industrial use. Na₂SiO₃ is a dense, sticky liquid that is clear to off white in color and has a faint odor. The water content of the sodium silicate was 55% by mass and their properties scheduled in Table 3 According to manufacturer.

Table 3 Sodium Silicate's Properties*

“Value”	“Description”
“Appearance”	hazy
“Specific Gravity”	“1.534 - 1.551”
“Density - 20° Baume”	“51 ±0.5”
“The SiO ₂ -Na ₂ O ratio”	“2.4 ±0.05”
“Viscosity 20 ° C (CPS)”	“600-1200”
“SiO ₂ % by weight”	“32-33”
“H ₂ O % by weight”	“55.1”
“Na ₂ O ₃ % by weight”	“13.1 - 13.7”

“*According to Manufacturer.”

2.1.6 Reinforcing Bars

The deformed bars that used throughout the present study are of 6mm and 8mm in diameter. The reinforcing steel testing results of such bars are listed in Table 4. Such tests are done according to American Testing Standard Measurements (ASTM) A615 within the laboratories of the Engineering Consulting Office / University of Al - Mustansiriyah.

Table 4 Tension tests results for steel bars within this study*

Nominal diameter mm	8	12
Normal diameter mm	7.89	11.983
Yield stress MPa	517	705
Yield strain mm/mm	0.00201	0.00211
Ultimate strength MPa	654	557
Ultimate strain mm/mm	0.167	0.171
Elongation %	10	9

*Engineering Consulting Office / University of Al - Mustansiriyah

2.2 Mix Proportions

Within the proposed experimental program, the mix design was taken from Abdul Aleem and Arumairaj, (2012) 10 . Table 5 lists the final mix proportioned that used in casting the specimens.

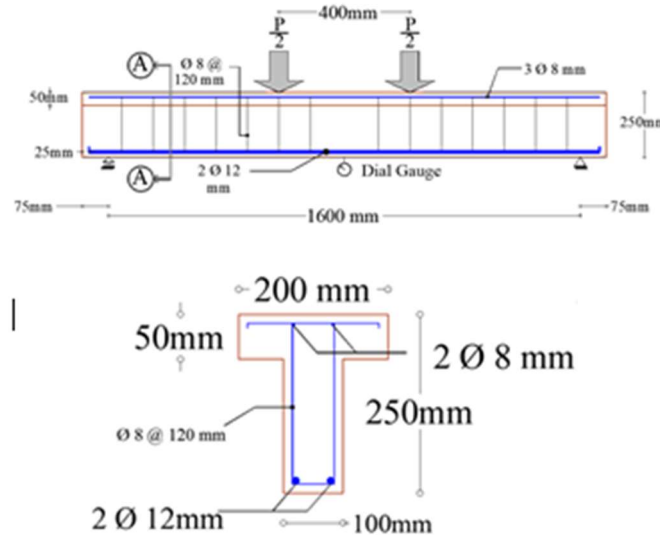
Tables 5 The mix proportions quantities per one cubic meter.

Material	Fly Ash	Sand	Gravel	Na ₂ SO ₃	10 Molar NaOH
Quantity (kg/m ³)	408	571.2	1305.6	103	41

2.3 Specimens Description and Study Variables

2.3.1 Specimen Description

All the tested beams within this experimental program are of center to center span of 1600 mm and 1750 mm total length. The section dimensions are of total height of 250mm and flange width of 200mm while the while the web width is 100mm. All the beams were reinforced by 2 ϕ 8mm top and 2 ϕ 12mm top bottom bars as a main reinforcement. In addition, ϕ 8mm stirrups were spaced @ 120mm from each end of beam as shown in Figure 3.



Section A – A

Figure 3. Specimen details of the present study

The specimen designation includes four digits, the first represented by “G” which means the “geopolymer concrete”. The second digit represented by either “C” which means “Circular” or by “S” which means “Square” or by “R” which means by “Rectangular”. The third digit represented by either “B” which refers to “Big” or by “S” which refers to “Small” opening. The fourth digit represented by either “S” which means “Single” or by “D” which means “Double”.

The experimental program of this study are consisted of five specimens, one of these are solid specimen and the other specimens are divided into groups, the first group is divided into two specimens, one of small circular opening (76.2mm in diameter) and the other is of big circular opening (101.6mm) as shown in Figure 4 a. The second group is divided into two specimens, one of small square opening (50mm x 50mm) and the other is of big square opening (66.3mm x 66.3mm) as shown in Figure 4 b. The third group is divided into two specimens. Finally, Table 5 shows the specimens map.

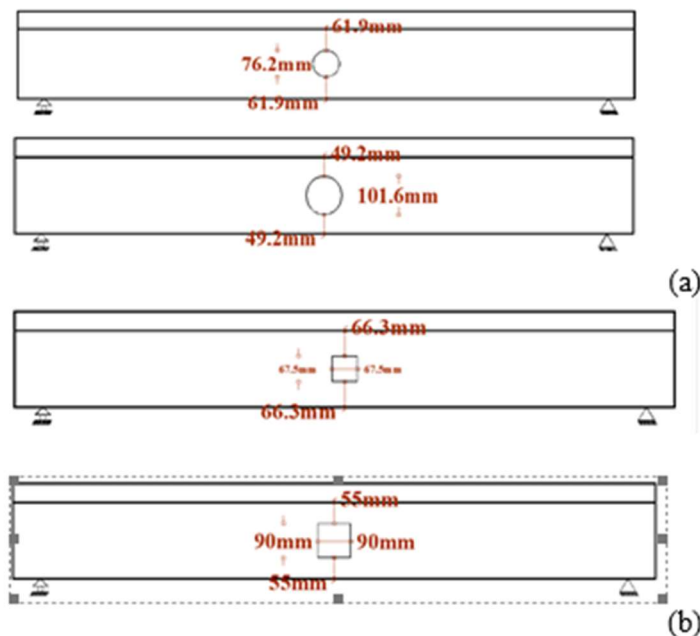


Figure 4. Groups map of the current study

Table 6 Specimens desination

Group	Designation	Description
/	Reference	Base line for comparison
Group one	GCSS	Geopolymer concrete with single small Circular opening
	GCBS	Geopolymer concrete with single big Circular opening
Group two	GSSS	Geopolymer concrete with single small square opening
	GSBS	Geopolymer concrete with single big square opening

2.3.2 Variables of This Study

The following are the variables that were considered in this study:

- 1) Size of circular and square transvers web opening.
- 2) The shape of the transverse web opening.

2.4 Molds of Specimens Mixing, Casting Procedure and Curing

The molds that were used for casting the specimens of the present experimental program are fabricated to facilitate the moving of its sides in addition to provide accurate dimensions for web and flange of the designed section. The inner dimensions of such molds are (flange width = 200mm flange depth= 50mm total section depth = 250mm and web width = 100mm) as illustrated previously.

2.5 Mixing, Casting and Curing Procedure

The 0.09 m³ rotary mixer illustrated in Figure 5 was used to complete the full mixing operation during this research program. The next procedure are followed to do sufficient mixing:

1. Prior to any subsequent mixing, the used mixer was thoroughly cleaned.
2. The molds were cleaned and oiled by suitable car engine oil to prepare it for casting.
3. The Na₂SiO₃ and NaOH solutions was prepared at the required molar concentrations before starting mixing process.
4. The sand, gravel and fly ash were mixed for 60 seconds.
5. The solution was added to the rotary and the mixing have taken 180 seconds.
6. The mixed quantity were casted to fill the molds and leveled with suitable trowel as shown in Figure 6.
7. The specimens was demolded after 24 hours to start curing under the laboratory ambient.



Figure 5. The used mixer



Figure 6. Leveling the casted specimens

2.6 Preliminary Mechanical Testing

2.6.1 “The Compressive Strength (f_c)”

This test was done to the GC cylindrical samples of 150mm x 300mm according to ASTM C 39/C 39 M15a, (2015). The testing machine that were used throughout this testing are of 6.8 kN/s loading rate and 3000 kN total capacity. This test was done at 28 days at the Laboratories of Civil Engineering Department /College of Engineering / University of Al Mustansiriya.

2.6.2 “Rupture Modulus (f_r)”

GC prisms was casted with dimensions of 500mm×100mm×100mm in with respect to ASTM C78/C78M – 15a, (2015). The total capacity of the testing machine was 50 kN and the required four point loading testing machine was done within the Laboratories of Civil Engineering Department /College of Engineering / University of Al Mustansiriya.

2.6.3 “Splitting Tensile Strength (f_{ct})”

This test was done at 28 days of age using GC cylindrical specimens with dimensions 150mm × 300mm according to ASTM C496/C496M – 11, (2011).

2.6.4 “Modulus of Elasticity”

This test has been achieved on the GC specimens of dimensions 150mm×300 mm at 28 days of age, to determine the elastic modulus of concrete specimens. The concrete cylinder subjected to 40% of ultimate compressive strength of samples in accordance with ASTM C469/C469M –14, (2014). Concrete’s modulus of elasticity has been estimated by the use of the stress-strain diagram for cylindrical specimens.

2.7 Testing Process

The comprehensive apparatus shown in Figure 7 was used to test all of the GC beam samples. Prior to the test, all samples were brushed and white-colored with appropriate paint to show the cracking paths that developed. Two concentrated loads were applied through a steel loading plate over a thin rubber strip which is used to get a suitable support. Just at start of the experiment, the initial readings of the dial gauge and the strain gauge were taken. The load was imposed in smaller steps in each of the

experiments and readings of deflection, strain and load were recorded in each increment. The load was gradually increased until failure.



Figure 7. Testing machine

2.7.1 Deflection Measurement

The vertical deflection was measured by dial gauge with an accuracy of 0.01mm that was positioned on the lower face of the mid-span of beams as shown Figure 8.



Figure 8. The 0.01mm accuracy dial gauge

2.7.2 Strain Measurements

The reinforcement strain has been measured with the use of the electrical strain gauge with a $120\ \Omega$ resistance and a $30\text{mm} \times 10\text{mm}$ and /or $40\text{mm} \times 10\text{mm}$ dimensions. Electrical wires were used to link the strain gauge cells to the computerized reading system shown in Figure 9. In addition, the strain gauges were installed in the tension steel “below the transverse web openings”, top extreme fiber of compression.

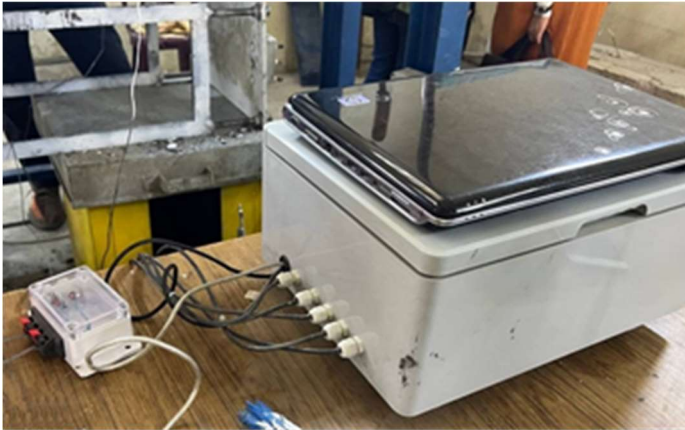


Figure 9. Data logger device (strain bridges reader)

3. Results

The structural behavior within the current study was represented by the first cracking load (P_{cr}), Service Load (P_s), and Load Carrying Capacity (P_u), Service Deflection (Δ_s) Maximum Deflection (Δ_m), the load strain response and the related cracking patterns.

3.1 P_{cr} , P_s and P_u

For the first group, Table 7 show the size effect of single circular transverse web opening to the P_{cr} , P_s and P_u of T – section geopolymer RC beams. The presence of small circular transverse web opening decreased the P_{cr} by 3.43% while the presence of big circular transverse web opening decreased the P_{cr} by 18.73%.

Turning to P_s , the presence of small circular transverse web opening decreased this value by 7.19% while the presence of big circular transverse web opening decreased the P_s by 11.30%. Regarding P_u , the presence of small circular transverse web opening decreased this value by 3.30% while the presence of big circular transverse web opening decreased the P_u by 11.21%.

The general purpose of the decreasing P_{cr} , P_s and P_u of T – section geopolymer RC beams is the presence of transverse web openings which leads to decrease the moment of inertia of the GC section. In addition, it can be extrapolated from these results that the effect of single circular size transverse web opening is more in P_{cr} than in P_s and P_u , this can be attributed to the fact that the GC have a serious share in bearing tension stresses at early stages (before first cracking). This share is decreased as the load is progressed after the first cracking occurrence.

Table 7 Size effect of single circular transverse web opening to P_{cr} , P_s and P_u of T – section geopolymer RC beams.

Designation	Reference	GCSS	GCBS
Pcr (kN)	12.55	12.12	10.2
Decrease in Pcr %	/	3.43	18.73
Ps (kN)	55.11	51.15	48.88
Decrease in Ps %	/	7.19	11.30
Pu (kN)	66	63.82	58.60
Decrease in Pu %	/	3.30	11.21

For the second group, Table 8 shows the size effect of single square transverse web opening to the Pcr, Ps and Pu of T – section geopolymer RC beams. The presence of small square transverse web opening decreased the Pcr by 3.98% while the presence of big square transverse web opening decreased the Pcr by 19.98%.

Furthermore, the presence of small square transverse web opening decreased Ps by 6.86% while the presence of big square transverse web opening decreased the Ps by 12.99%. For Pu, the presence of small square transverse web opening decreased this value by 4.32% while the presence of big square transverse web opening decreased the Pu by 12.30%.

In general, the purpose of lack in performance square transverse web opening can be also ascribed to the lack in moment of inertia within GC section as in the previous group.

Comparing these results with the first group reveals that Pcr, Ps and Pu of square transverse web opening are less than those of circular for each even with comparing the same size of openings. This can be attributed to the fact that the change in GC section is abrupt in nature in square openings while it is gradual in circular openings.

The effect of changing size of square transverse web opening is still more in Pcr than in Ps and Pu for the same purpose that mentioned in the previous group.

Table 8 Size effect of single square transverse web opening to Pcr, Ps and Pu of T – section geopolymer RC beams.

Designation	Reference	GSSS	GSBS
Pcr (kN)	12.55	12.05	10.05
Decrease in Pcr %	/	3.98	19.98
Ps (kN)	55.11	51.33	47.95
Decrease in Ps %	/	6.86	12.99
Pu (kN)	66	63.15	57.88
Decrease in Pu %	/	4.32	12.30

3.2 Service Deflection Δ_s Maximum Deflection Δ_m and The Relevant Load Deflection Curves

For the first group, Table 9 shows the size effect of single circular transverse web opening to the Δ_s and Δ_m of T – section geopolymer RC beams. The existence of small circular transverse web opening increased the Δ_s by 4.55% while the presence of big circular transverse web opening increased the Δ_s by 9.09%.

It is also apparent from that table that the existence of small circular transverse web opening decreased the Δ_m by 2.1 % while the presence of big circular transverse web opening increased the Δ_m by 3.2%.

The Δ_s decreased as the size of circular transverse web opening is increased while the vice versa is existed in Δ_m . This pointed that the deflection is propagated rapidly before and after service limits which means that as the size of opening is high, the deflection limits at service load and at fracture (corresponding to load carrying capacity) are early to appear.

Figure 10 shows the load deflection diagram of the Reference, GCSS and GCBS respectively, it can be noticed within that figure that the first phase (Phase I) is the elastic one till reaching the first cracking limit. At the end of this limit, the cracks will be appeared clearly. The second Phase (Phase II) begins after the first cracking load when the begin to be more in number and cracking width is progressed more and more till the P_s . after this limit, the last phase (Phase III) is usually begun which included more cracking width and the final fracture at the end of load capacity of beam.

It can be noticed also from that figure that the curves have approximately the same paths till about 20 kN of load, after that, there are clear deviation of these paths. This is because of the concrete can withstand stress before 20 kN and its reduction will be more clear as the load after this load when the steel reinforcement begun to withstand more stress to compensate this reduction of concrete.

In addition, it is also clear that the stiffness of the geopolymer RC beams that have single transverse web openings have lower stiffness than solid once. However, this matter is characterized and discussed next section.

Table 9 Size effect of single circular transverse web opening to Δ_s and Δ_m of T – section geopolymer RC beams.

Designation	Reference	GCSS	GCBS
Δ_s mm	3.3	3.45	3.60
Increase in Δ_s %	/	4.55	9.09
Δ_m mm	14.3	14	13.84
Decrease in Δ_m %	/	2.1	3.2

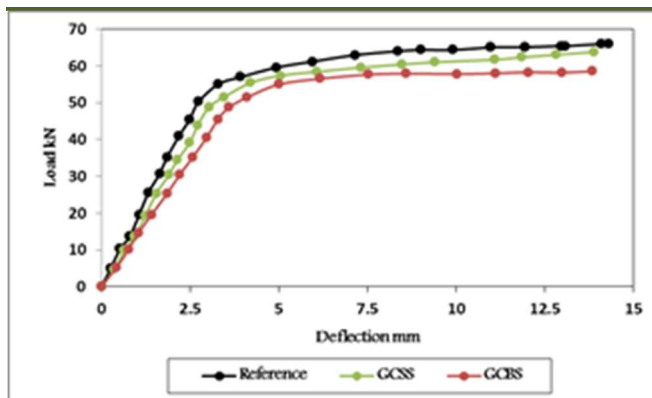


Figure 10. Size effect of single circular transverse web opening to load deflection response limits of T – section geopolymer RC beams.

For the second group, Table 10 shows the size effect of single square transverse web opening to the Δ_s and Δ_m of T – section geopolymer RC beams. The presence of small square transverse web opening increased the Δ_s by 5.76% while the presence of big square transverse web opening increased the Δ_s by 9.70%.

As that table shows, the existence of small circular transverse web opening decreased the Δm by 3.85% while the presence of big circular transverse web opening increased the Δm by 6.71%.

As in the first group, Δs decreased as the size of transverse web opening is increased while Δm is decreased due to the same purposed mentioned within the first group.

Together these results with the first group, it is apparent the Δs of the square transverse web opening is more than those of square transverse web opening for the same corresponding size. This is because the first cracking occurrence is earlier and the consequent propagation of cracking at the service load is also early to be detected.

In addition, the Δm of the square transverse web opening is less than those of square transverse web opening for the same corresponding size. This can be attributed to the fact that the early dissipation of links between concrete fragments at the post service load phase due to the early cracking propagation. In addition, Figure 11 shows the load deflection diagram of the Reference, GSSS and GSBS respectively, it can be noticed that the observed phases of load deflection curves are the same of the first group which are Phase I (elastic phase till the P_{cr} limit), Phase II (from P_{cr} to P_s and Phase III (from P_s to P_u).

As in the previous group, the load – deflection curves have approximately the same path before 20 kN of load and begin to illustrate more deviation after that load due to the same purpose discussed earlier. Moreover, a deep vision to the load deflection curves reveals that the geopolymer RC beams that have single square transverse web openings have lower stiffness, ductility than reference as in group one. Table 10 Size effect of single square transverse web opening to Δs and Δm of T – section geopolymer RC beams.

Designation	Reference	GSSS	GSBS
Δs mm	3.3	3.49	3.62
Increase in Δs %	/	5.76	9.70
Δm mm	14.3	13.75	13.34
Decrease in Δm %	/	3.85	6.71

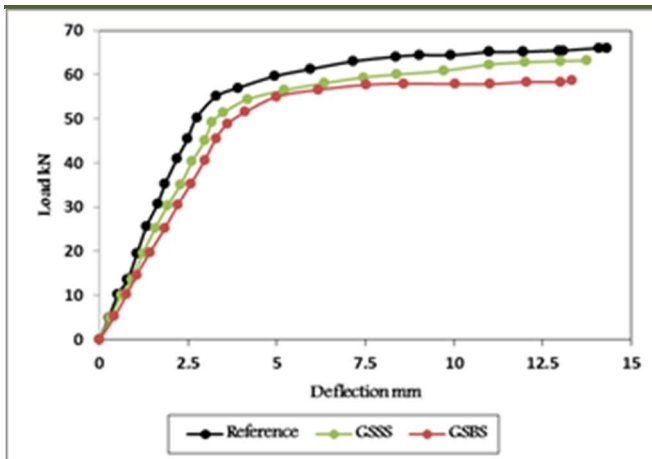


Figure 11. Size effect of single square transverse web opening to load deflection response limits of T – section geopolymer RC beams.

3.3 Load Strain Diagrams

For the first group, Table 11 and Figure 12 show the Size effect of single circular transverse web opening to load – tension steel strain behavior of T – section geopolymer RC beams. While Table 12 and Figure 13 show this effect to load concrete compressive strain behavior.

From data in Table 11, single small circular transverse web opening increased service tension steel strain ϵ_{st} and maximum tension steel strain ϵ_{mt} by 2.96% and 4.17% respectively while the presence of big circular transverse web opening decreased ϵ_{st} and ϵ_{mt} by 18.23% and 6.51% respectively. These results showed that there are a reasonable hierarchy between the load deflection and load strain response which can be considered as an affirmative for the previous outcomes. The recorded levels of ϵ_{st} are near the known levels of steel reinforcement yielding.

Turning to Table 12, it is apparent that the maximum concrete compressive strain (ϵ_{mc}) increased as the reduction in concrete increased which is also representing an expected result because the compressive concrete should have a share in compensating concrete reduction. However, single small circular transverse web opening increased maximum compressive concrete strain (ϵ_{mc}) by 4.17% while the presence of single big circular transverse web opening decreased ϵ_{mc} 6.51%. The recorded levels of compressive concrete is less than the known crushing levels of GC.

Table 11 Size effect of single circular transverse web opening to tension steel strain of T – section geopolymer RC beams.

Designation	Reference	GCSS	GCBS
ϵ_{st}	0.00203	0.00209	0.00240
Increase ϵ_{st} %	/	2.96	18.23
ϵ_{mt}	0.00384	0.00368	0.00359
Decrease in ϵ_{mt} %	/	4.17	6.51

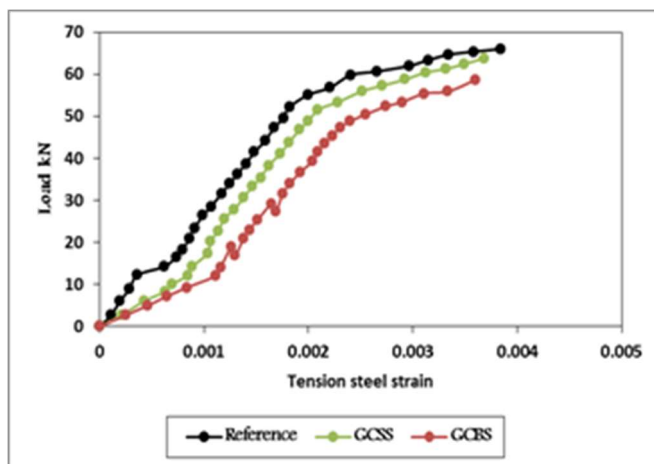


Figure 12. Size effect of single circular transverse web opening to tension steel strain response of T – section geopolymer RC beams.

Designation	Reference	GCSS	GCBS
-------------	-----------	------	------

ϵ_{mc}	0.00193	0.00200	0.00208
Increase in ϵ_{mc} %	/	3.63	7.77

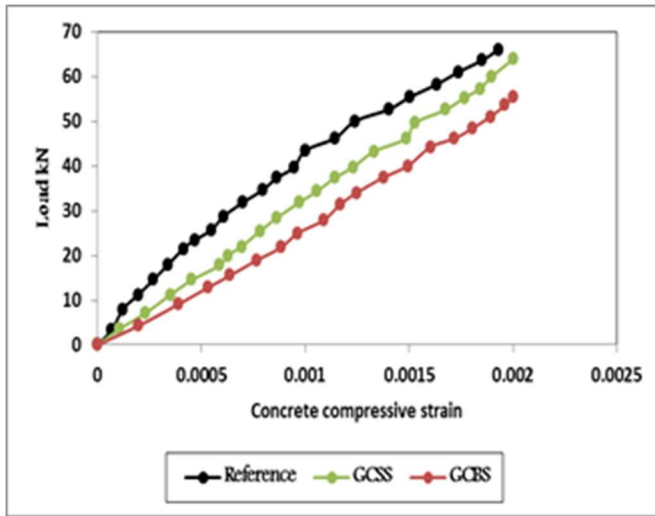


Figure 13. Size effect of single circular transverse web opening to compressive concrete strain response of T – section geopolymer RC beams.

For the second group, Table 13 and Figure 14 show the Size effect of single square transverse web opening to load – tension steel strain behavior of T – section geopolymer RC beams. While Table 14 and Figure 15 show this effect to load concrete compressive strain behavior.

As listed in Table 13, single square circular transverse web opening increased service ϵ_{st} and ϵ_{mt} by 10.84% and 6.51% respectively while the presence of big square transverse web opening decreased ϵ_{st} and ϵ_{mt} by 23.16% and 9.11% respectively.

As in the previous group, the same hierarchical order is observed between the load deflection and the load strain response. In addition, ϵ_{st} levels is also near the yielding limit of steel reinforcement as described previously.

The ϵ_{st} levels of this group is more than the first group and vice versa for ϵ_{mt} as an expected outcome to the intended hierarchy for the same size of openings. For Table 14, it is obvious that the ϵ_{mc} increased as the reduction in concrete increased as in the previous group. However, single small square transverse web opening increased ϵ_{mc} by 6.51% while the presence of single big square transverse web opening decreased ϵ_{mc} 9.11%.

Table 13 Size effect of square circular transverse web opening to tension steel strain of T – section geopolymer RC beams.

Designation	Reference	GSSS	GSBS
ϵ_{st}	0.00203	0.00225	0.00250
Increase ϵ_{st} %	/	10.84	23.16
ϵ_{mt}	0.00384	0.00359	0.00339

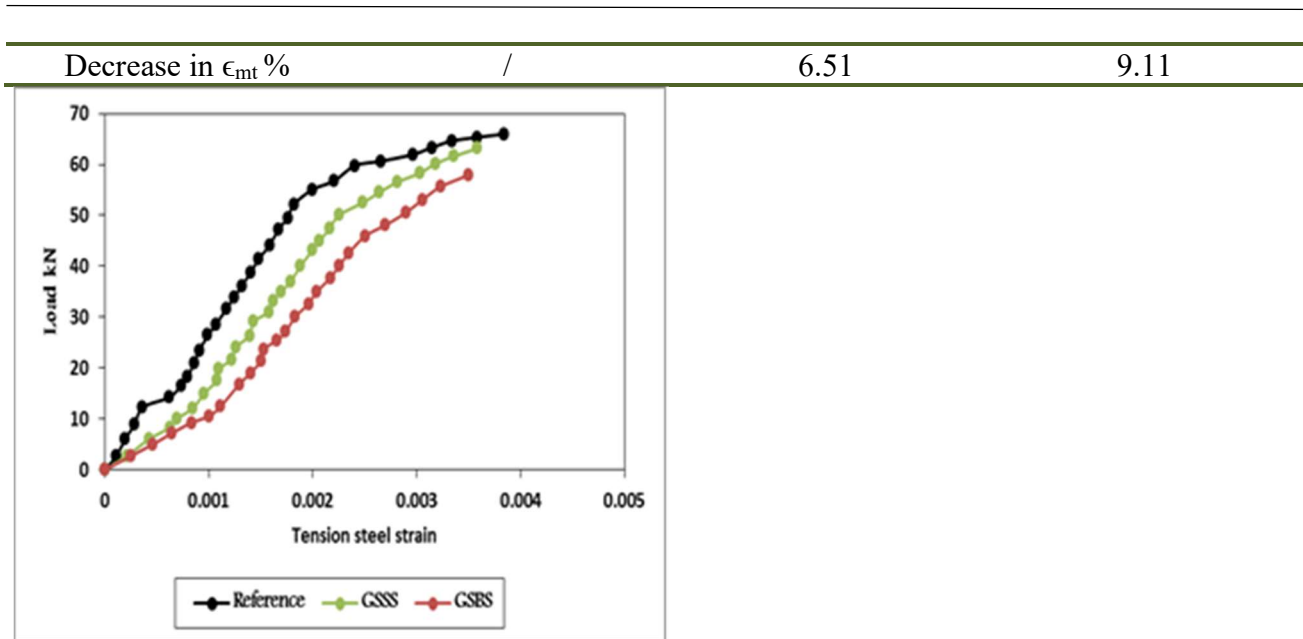


Figure 14. Size effect of single square transverse web opening to tension steel strain response of T – section geopolymer RC beams.

Table 12 Size effect of single square transverse web opening to compressive concrete strain of T – section geopolymer RC beams.

Designation	Reference	GSSS	GSBS
ϵ_{mc}	0.00193	0.00195	0.00204
Increase in ϵ_{mc} %	/	1.04	5.70

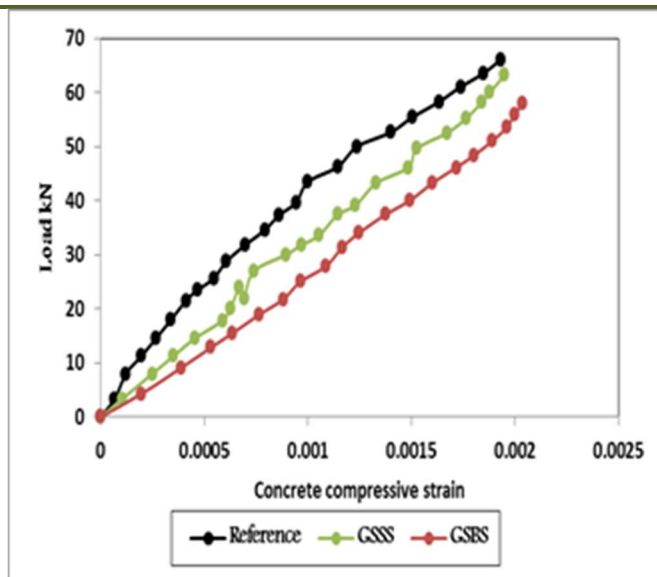


Figure 15. Size effect of single square transverse web opening to compressive concrete strain response of T – section geopolymer RC beams.

2.4 Cracking Propagation and Mode of Failure

The mode of failure of all the specimens within the first group is the "flexural" as shown in Figure 16. In general, the cracks numbers in GCSS is less than GCBS. In addition, these cracks did not propagated within the flange of the GCSS as in the GCBS. However, this order between specimens confirms the order between them with respect to ϵ_{mc} . Finally, for both specimens within this group, no STM nor any relevant plastic hinges were appeared. This conforms that the beam theory does not be broken under the proposed circumstances.



Figure 16. Size effect of single circular transverse web opening to the mode of square and cracking propagation of T – section geopolymer RC beams.

For the second group and as in the previous group, mode of failure of all the specimens is the "flexural" as shown in Figure 17. Additionally, the cracks numbers in GSSS are also less than GSBS (as in Group one). However, the cracks are propagated in both specimens at the flange but are more in number in GSBS. The same extrapolated compatibility with ϵ_{mc} can be seen also within this group. No STM nor any relevant plastic hinges were appeared as in in group one and the same not regarding beam theory was reported.



Figure 17. Size effect of single circular transverse web opening to the mode of square and cracking propagation of T – section geopolymer RC beams.

4. Conclusions

The Following conclusions can be drawn from this study:

- 1) The presence of transverse web opening at the center of geopolymer RC beams can cause a consequent lack in structural behavior.
- 2) The load deflection response of geopolymer T beams is similar to conventional RC beams.
- 3) The presence of transverse web openings reduce the first cracking load, yielding load and maximum load carrying capacity.
- 4) The general performance of geopolymer T beams that have circular transverse web openings perform better than those that have square transverse web opening.
- 5) Further research is needed to include the rectangular transverse web openings.
- 6) Future research should be devoted to investigate the effect of the presence of transvers web openings at the effective shear zone.
- 7) the effect of the presence of transvers web openings at the effective shear zone.

5. References

- 1) Dattatreya J. K. and Rajamane N.(2011) P. (2011) "Flexural Behavior of Reinforced Geopolymer Concrete Beams," International journal of civil and structural engineering, Vol. 2, No. 1, pp: 138-159.
- 2) Kumar B.S.H and K. Ramesh. (2018). "Analytical Study on Flexural Behaviour of Reinforced Geopolymer Concrete Beams by ANSYS." IOP Conference Series: Materials Science and Engineering. Vol. 455, No. 1.
- 3) Rangan B. V. (2010) "Fly Ash-Based Geopolymer Concrete," Proceedings of the International Workshop on Geopolymer Cement and Concrete, Allied Publishers Private Limited, 2010.
- 4) Singh B., Ishwarya G., Gupta M., and Bhattacharyya S.K., (2015) "Geopolymer concrete: A review of some recent developments" Construction and Building Materials Vol. 85, pp: 78–90.
- 5) Li C, Sun H, and Li L.(2010) "A review the comparison between alkali-activated slag (Si+Ca) and metakaolin (Si+Al) cements" Cement and Concrete Research. Vol. No. 9., pp: 1341–1349.
- 6) BS EN 196-2:2013 Method of testing cement Chemical analysis of cement.
- 7) Iraqi Specifications No. (5). Portland cement. Baghdad, Iraq. "Iraqi Central Organization for Standardization and Quality Control". Planning Council, Baghdad, Iraq. 1984.
- 8) BS 882:1992 Specification for aggregates from natural sources for concrete (AMD 13579).
- 9) ASTM A 615/A 615M . Standard Specification for Deformed and Plain Billet-Steel Bars for Concrete Reinforcement. American Society for Testing and Materials. 2013.
- 10) Aleem, Abdul & Arumairaj, P.D.. (2012). Optimum mix for the geopolymer concrete. Indian Journal of Science and Technology. 5. 2299-2301. 10.17485/ijst2012v5i3.8.
- 11) FA: Hersh F. Mahmood, Hooshang Dabbagh, Azad A. Mohammed, Comparative study on using chemical and natural admixtures (grape and mulberry extracts) for concrete, Case Studies in Construction Materials, Volume 15, 2021,
- 12) Kumar, S. (2022). A quest for sustainium (sustainability Premium): review of sustainable bonds. Academy of Accounting and Financial Studies Journal, Vol. 26, no.2, pp. 1-18
- 13) Allugunti, V.R. (2019). Diabetes Kaggle Dataset Adequacy Scrutiny using Factor Exploration and Correlation. International Journal of Recent Technology and Engineering, Volume-8, Issue-1S4, pp 1105-1110.

- 14) ASTM C39/C39M “Standard Test Method for Compressive Strength of Cylindrical Concrete Specimens. American Society for Testing and Materials”.
- 15) ASTM C78 “Standard Test Method for Flexural Strength of Concrete (Using Simple Beam with Third-Point Loading). American Society for Testing and Material”. 2015.
- 16) ASTM C469-14, “Standard Test Method for Static Modulus of Elasticity and Poisson’s Ratio of Concrete in Compression”, 2014.